

Magnetic Nanostructures and Spintronics, Fig. 7 Hard disk media magnetic domain structure. On the *left* conventional media for perpendicular recording, with randomly distributed magnetic domains and irregular bit contour. On the *right* patterned media, where each nanostructured element may carry one single bit of information

assembly guided by the underlying chemically modified former pattern [15]. Large area-patterned nanostructures are studied also for their interesting collective behavior [16], resulting in peculiar electrical properties [17] and potentially suitable to implement full magnetic logics, particularly promising for their low electrical consumption [18].

Cross-References

- ▶ [Chemical Vapor Deposition \(CVD\)](#)
- ▶ [Electron Beam Lithography \(EBL\)](#)
- ▶ [Nanoparticles](#)
- ▶ [Physical Vapor Deposition](#)
- ▶ [Self-Assembly of Nanostructures](#)

References

1. Sander, D.: The magnetic anisotropy and spin reorientation of nanostructures and nanoscale films. *J. Phys. Condens. Matter* **16**, R603–R636 (2004)
2. Nogues, J., Schuller, I.K.: Exchange bias. *J. Magn. Magn. Mater.* **192**, 203–232 (1999)
3. Chiolerio, A., Allia, P., Chiodoni, A., Pirri, F., Celegato, F., Coisson, M.: Thermally evaporated Cu-Co top spin-valve with random exchange bias. *J. Appl. Phys.* **101**, 123915-1–123915-6 (2007)
4. Berkowitz, A.E., Takano, K.: Exchange anisotropy – a review. *J. Magn. Magn. Mater.* **200**, 552–570 (1999)

5. Parkin, S.S.P.: Giant magnetoresistance in magnetic nanostructures. *Annu. Rev. Mater. Sci.* **25**, 357–388 (1995)
6. Yuasa, S., Djayapavira, D.D.: Giant tunnel magnetoresistance in magnetic tunnel junctions with a crystalline MgO (001) barrier. *J. Phys. D Appl. Phys.* **40**, R337–R354 (2007)
7. Slonczewski, J.C.: Current-driven excitation of magnetic multilayers. *J. Magn. Magn. Mater.* **159**, L1–L7 (1996)
8. Ralph, D.C., Stiles, M.D.: Spin transfer torques. *J. Magn. Magn. Mater.* **320**, 1190–1216 (2008)
9. Cros, V., Boulle, O., Grollier, J., Hamzic, A., Munoz, M., Pereira, L.G., Petroff, F.: Spin transfer torque: a new method to excite or reverse a magnetization. *C.R. Physique* **6**, 956–965 (2005)
10. Sun, Z.: Spin angular momentum transfer in current-perpendicular nanomagnetic junctions. *IBM J. Res. Dev.* **50**, 81–100 (2006)
11. Wang, X., Chen, Y.: Spintronic memristor devices and application. In: *Proceedings of Design, Automation & Test in Europe Conference & Exhibition (DATE)*, IEEE Conferences, Dresden, pp. 667–672 (2010)
12. Schmidt, J.: Concepts for spin injection into semiconductors—a review. *J. Phys. D Appl. Phys.* **38**, R107–R122 (2005)
13. Awschalom, D.D., Flatté, M.E.: Challenges for semiconductor spintronics. *Nat. Phys.* **3**, 153–159 (2007)
14. Dietzel, A.: Hard disk drives. In: Waser, R. (ed.) *Nanoelectronics and Information Technology*, 2nd edn, pp. 617–629. Wiley, Weinheim (2005)
15. Density multiplication and improved lithography by directed block copolymer assembly for patterned media at 1 Tbit/in² and beyond, white paper WPD08EN-01, Hitachi GST, San Jose, CA (2008)
16. Adeyeye, A.O., Singh, N.: Large area patterned magnetic nanostructures. *J. Phys. D Appl. Phys.* **41**, 153001-1–153001-29 (2008)
17. Chiolerio, A., Allia, P., Celasco, E., Martino, P., Spizzo, F., Celegato, F.: Magnetoresistance anisotropy in a hexagonal lattice of Co antidots obtained by thermal evaporation. *J. Magn. Magn. Mater.* **322**, 1409–1412 (2010)
18. Graziano, M., Vacca, M., Chiolerio, A., Zamboni, M.: An NCL-HDL snake-clock-based magnetic QCA architecture. *IEEE Trans. Nanotech.* **10**, 1141–1149 (2011)

Magnetic Resonance Force Microscopy

Martino Poggio¹ and Christian L. Degen²

¹Department of Physics, University of Basel, Basel, Switzerland

²Department of Physics, ETH Zurich, Zurich, Switzerland

Synonyms

[Force-detected magnetic resonance](#)

Definition

Magnetic resonance force microscopy (MRFM) is a type of magnetic resonance imaging (MRI) now capable of acquiring three-dimensional (3D) images of tiny samples with a spatial resolution better than 10 nm. By applying the techniques of scanning probe microscopy (SPM), MRFM surpasses the sensitivity of conventional, inductive MRI by eight orders of magnitude. MRFM images the interior of nanoscale objects noninvasively and with intrinsic chemical selectivity and, in 2009, it was used to capture 3D images of individual virus particles.

Overview

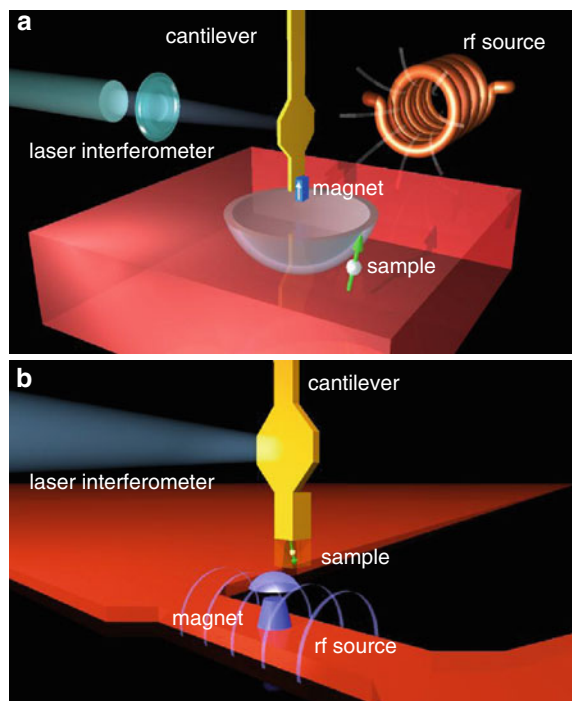
MRFM relies on the mechanical measurement of the weak magnetic force between a microscopic magnet and the magnetic moments in a sample. These moments are due to either the atomic nuclei with nonzero nuclear spin or electron spins present in a sample. For a single magnetic moment $\boldsymbol{\mu}$ in a magnetic field \mathbf{B} , this force can be expressed as:

$$\mathbf{F} = \nabla(\boldsymbol{\mu} \cdot \mathbf{B}). \quad (1)$$

Using a compliant cantilever, one can measure the component of \mathbf{F} along the cantilever's deflection direction \hat{x} :

$$F_x = \frac{\partial}{\partial x}(\boldsymbol{\mu} \cdot \mathbf{B}) = \mu \frac{\partial B_z}{\partial x} = \mu G, \quad (2)$$

where $\boldsymbol{\mu}$ points along \hat{z} and $G = \frac{\partial B_z}{\partial x}$ is a magnetic field gradient. First, either the sample containing nuclear or electronic moments or the nano-magnet must be fixed to the cantilever. The sample and magnet must be in close proximity, sometimes up to a few tens of nanometers from each other. A nearby radiofrequency (rf) source produces magnetic field pulses similar to those used in conventional MRI, causing the moments to periodically flip. This periodic inversion generates an oscillating magnetic force acting on the cantilever. In order to resonantly excite the cantilever, the magnetic moments can be inverted at the cantilever's mechanical resonance frequency. The cantilever's mechanical oscillations are then measured by an optical interferometer or beam deflection detector. The electronic



Magnetic Resonance Force Microscopy, Fig. 1 Schematics of an MRFM apparatus. (a) Corresponds to the “tip-on-cantilever” arrangement, such as used in the single-electron MRFM experiment of 2004 [1]. (b) Corresponds to the “sample-on-cantilever” arrangement, like the one used for the nanoscale virus imaging experiment in 2008 [2]

signal produced by the optical detector is proportional to the cantilever oscillation amplitude, which depends on the number of moments in the imaging volume. Spatial resolution results from the fact that the nano-magnet produces a magnetic field which is a strong function of position. The magnetic resonance condition and therefore the region in which the spins periodically flip is confined to a thin, approximately hemispherical “resonant slice” that extends outward from the nano-magnet (see Figs. 1 and 4). By scanning the sample in 3D through this resonant region, a spatial map of the magnetic moment density can be made. Different types of magnetic moments (e.g., ^1H , ^{13}C , ^{19}F , or even electrons) can be distinguished due to their different magnetic resonance frequencies, giving an additional chemical contrast.

In conventional nuclear magnetic resonance detection, the sample is placed in a strong static magnetic field in order to produce a Zeeman splitting between spin states. The sample is then exposed to an rf magnetic field of a precisely defined frequency. If this frequency

matches the Zeeman splitting, then the system absorbs energy from the rf radiation resulting in transitions between the spin states. The resulting oscillations of this ensemble of magnetic moments produce a time-varying magnetic signal that can be detected with a pickup coil. The electric current induced in the coil is then amplified and converted into a signal that is proportional to the number of moments (or spins) in the sample. In MRI this signal can be reconstructed into a 3D image of the sample using spatially varying magnetic fields and Fourier transform techniques. The magnetic fields produced by nuclear moments are, however, extremely small: more than one trillion (10^{12}) nuclear spins are typically needed to generate a detectable signal.

The advantage of force-detected over inductive techniques is that much smaller samples can be measured. In the latter case, the measurement can only be sensitive if the spins significantly alter the magnetic field within the pickup coil, i.e., if the spins fill a significant fraction of the coil volume. For spin ensembles with volumes significantly smaller than $(1\ \mu\text{m})^3$, it is extremely challenging to realize pickup coils small enough to ensure an adequate filling factor. As a result, even the best resolutions achieved by inductively detected MRI require sample volumes of at least $(3\ \mu\text{m})^3$ [3]. Mechanical resonators, in contrast, can now be fabricated with dimensions far below a micron, such that the sample's mass (which is the equivalent to the filling volume in a pickup coil) is always significant compared to the bare resonator mass. In addition, mechanical devices usually show resonant quality factors that surpass those of inductive circuits by orders of magnitude, resulting in a much lower baseline noise. For example, state-of-the-art cantilever force transducers achieve quality factors between 10^4 and 10^7 , enabling the detection of forces of $\text{aN/Hz}^{1/2}$ – less than a billionth of the force needed to break a single chemical bond. In addition, scanning probe microscopy offers the stability to position and image samples with nanometer precision. The combination of these features allows mechanically detected MRI to image at resolutions that are far below $1\ \mu\text{m}$ and – in principle – to aspire to atomic resolution.

Basic Methodology

Despite the large magnetic field gradients produced by specially made magnetic tips, the forces produced by

small number of magnetic moments remain astoundingly small: in an achievable gradient of $10^6\ \text{T/m}$, a single ^1H moment, for example, produces a force of about $10^{-20}\ \text{N}$. In order to detect forces due to small ensembles of moments, the most sensitive MRFM takes advantage of the thermally limited force resolution of specially made nanomechanical cantilevers. In addition, it utilizes the fact that the force of interest can be made to occur in a narrow bandwidth around the cantilever's mechanical resonance.

The sensitivity and resolution of MRFM hinge on a simple signal-to-noise ratio, which is given by the ratio of the magnetic force power exerted on the cantilever over the force noise power of the cantilever device. For small enough volumes of spins, one must measure statistical spin polarizations; therefore one is interested in force powers (or variances) rather than force amplitudes:

$$\text{SNR} = N \frac{(\mu G)^2}{S_F \Delta f}. \quad (3)$$

Here, N is the number of spins in the detection volume, μ is the magnetic moment of the relevant spin, G is the relevant magnetic field gradient at the position of the sample, S_F is the force noise spectral density set by the fluctuations of the cantilever sensor, and Δf is the bandwidth of the measurement, determined by the spin relaxation rate. This expression gives the single-shot signal-to-noise ratio of a thermally limited MRFM apparatus. The larger this signal-to-noise ratio is, the better the spin sensitivity will be.

From the four parameters appearing in (3), only two can be controlled and possibly improved. On the one hand, the magnetic field gradient G can be enhanced by using higher quality magnetic tips and by bringing the sample closer to these tips. On the other hand, the force noise spectral density S_F can be reduced by going to lower temperatures and by making intrinsically more sensitive mechanical transducers.

Key Findings

The use of force-detection techniques in nuclear magnetic resonance (NMR) experiments dates back to Evans in 1955 [4], and was also used in torque magnetometry measurements by Alzetta and coworkers in the

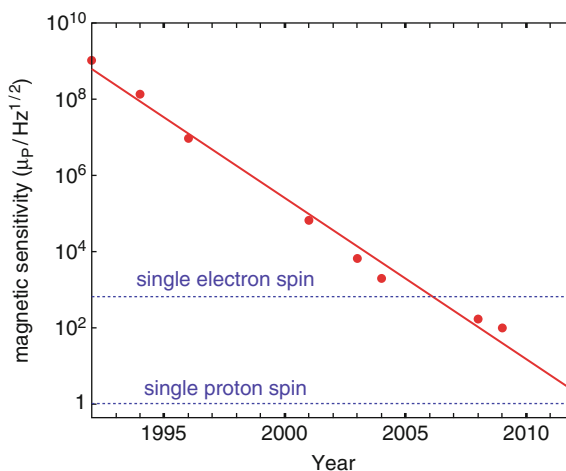
1960s [5]. In 1991, Sidles, independent of this very early work, realized that highly sensitive magnetic resonance detection could be achieved using microfabricated cantilevers and nanoscale ferromagnets. In these early days of scanning probe microscopy, he proposed the MRFM technique as a method to improve the resolution of MRI to molecular length scales [6, 7]. Subsequently, the first micrometer-scale experimental demonstration using cantilevers was realized by Rugar [8], demonstrating mechanically detected electron spin resonance in a 30-ng sample of diphenylpicrylhydrazyl (DPPH).

The visionary goal of the MRFM proposal was to eventually image molecules atom by atom, so as to directly map the 3D atomic structure of macromolecules [9]. Such a “molecular structure microscope” would have a dramatic impact on modern structural biology, and would be an important tool for many future nanoscale technologies. While this ultimate goal has not been achieved to date, the technique has undergone a remarkable development into one of the most sensitive spin detection methods available to researchers today. Among the important experimental achievements are the detection of a single electronic spin [1] and the extension of the spatial resolution of MRI from several micrometers to below 10 nm [2].

First Demonstration

The first MRFM apparatus operated in vacuum and at room temperature with the DPPH sample attached to the cantilever. A millimeter-sized coil produced an rf magnetic field tuned to the electron spin resonance of the DPPH (220 MHz) with a magnitude of 1 mT. By changing the strength of a polarizing magnetic field (8 mT) in time, the electron spin magnetization in the DPPH was modulated. In a magnetic field gradient of 60 T/m, produced by a nearby NdFeB permanent magnet, the sample’s oscillating magnetization resulted in a time-varying force between the sample and the magnet. This force modulation was converted into mechanical vibration by the compliant cantilever. Displacement oscillations were detected by a fiber-optic interferometer achieving a thermally limited force sensitivity of $3 \text{ fN}/\sqrt{\text{Hz}}$.

During the years following this initial demonstration of cantilever-based magnetic resonance detection, the technique has undergone a series of developments toward higher sensitivities that, as of today, is about 10^7 times that of the 1992 experiment (see Fig. 2). The

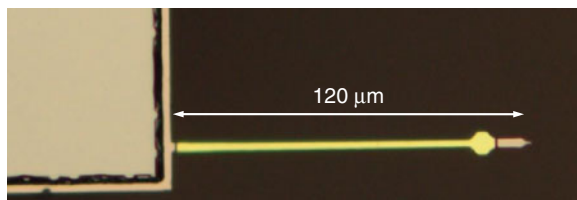


Magnetic Resonance Force Microscopy, Fig. 2 Advances to the sensitivity in force-detected magnetic resonance over time. Remarkably, improvements have closely followed a “Moore’s law” for over a decade, with the magnetic moment sensitivity doubling roughly every 8 months. Dots are experimental values [1, 2, 8, 10–14], and dashed lines indicate sensitivities of one electron and one proton magnetic moment (μp), respectively

following touches on two important demonstrations during this development. Several review articles and book chapters have appeared in the literature that discuss the historical progress of the technique more broadly and in richer detail [15–22].

Single-Electron MRFM

The measurement of a single electron spin by Rugar et al. in 2004 concluded a decade of development on the MRFM technique and stands out as one of the first single-spin measurements in solid-state physics. A variety of developments led to the exceptional measurement sensitivity required for single-spin detection. These include the operation of the apparatus at cryogenic temperatures and high vacuum, the ion-beam milling of magnetic tips in order to produce large gradients, and the fabrication of mass-loaded attonewton-sensitive cantilevers [23] (shown in Fig. 3). The thermal noise in higher order vibrational modes of mass-loaded cantilevers is suppressed compared with the noise in the higher order modes of conventional, “flat” cantilevers. Since high-frequency vibrational noise in combination with a magnetic field gradient can disturb the electron spin, the mass-loaded levers proved to be a crucial advance for single-electron MRFM. In addition, Rugar et al. developed a sensitive interferometer employing only a few



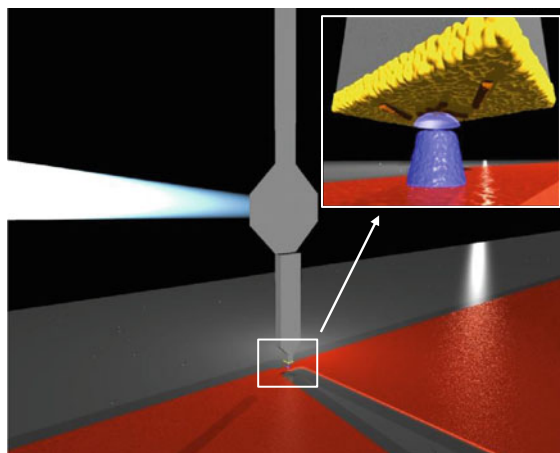
Magnetic Resonance Force Microscopy, Fig. 3 Image of an ultrasensitive mass-loaded Si cantilever taken from an optical microscope. This type of cantilever, which has a spring constant under $100 \mu\text{N/m}$, has been used as a force transducer in the many of the latest MRFM experiments [23]

nanowatts of optical power for the detection of cantilever displacement [24]. This low incident laser power is crucial for achieving low cantilever temperatures and thus minimizing the effects of thermal force noise. A low-background measurement protocol called OSCAR based on the NMR technique of adiabatic rapid passage was also employed [10]. Finally, the experiment required the construction of an extremely stable measurement system capable of continuously measuring for several days in an experiment whose single-shot signal-to-noise ratio was just 0.06 [1].

Nano-MRI

The detection of a single nuclear spin is far more challenging than that of single electron spin. The intrinsic magnetic moment of a nucleus is much smaller than that of an electron; as a result the force produced by a nuclear moment in (2) is proportionally smaller. A ^1H nucleus (proton), for example, possess a magnetic moment that is only $\sim 1/650$ of an electron spin moment. Other important nuclei, like ^{13}C or a variety of isotopes present in semiconductors, have even weaker magnetic moments. In order to observe single nuclear spins, it is necessary to improve the state-of-the-art sensitivity by another two to three orders of magnitude. While not out of the question, this is a daunting task that requires significant advances to all aspects of the MRFM technique. Despite these challenges, significant progress has been made. In particular, one experiment that used single tobacco mosaic virus (TMV) particles as the sample shows both the feasibility of MRI imaging with nanometer resolution and the applicability of MRFM to biologically relevant samples.

Figure 4 is a representation of the MRFM apparatus used in the experiment. The virus particles were transferred to the cantilever end by dipping the tip of the



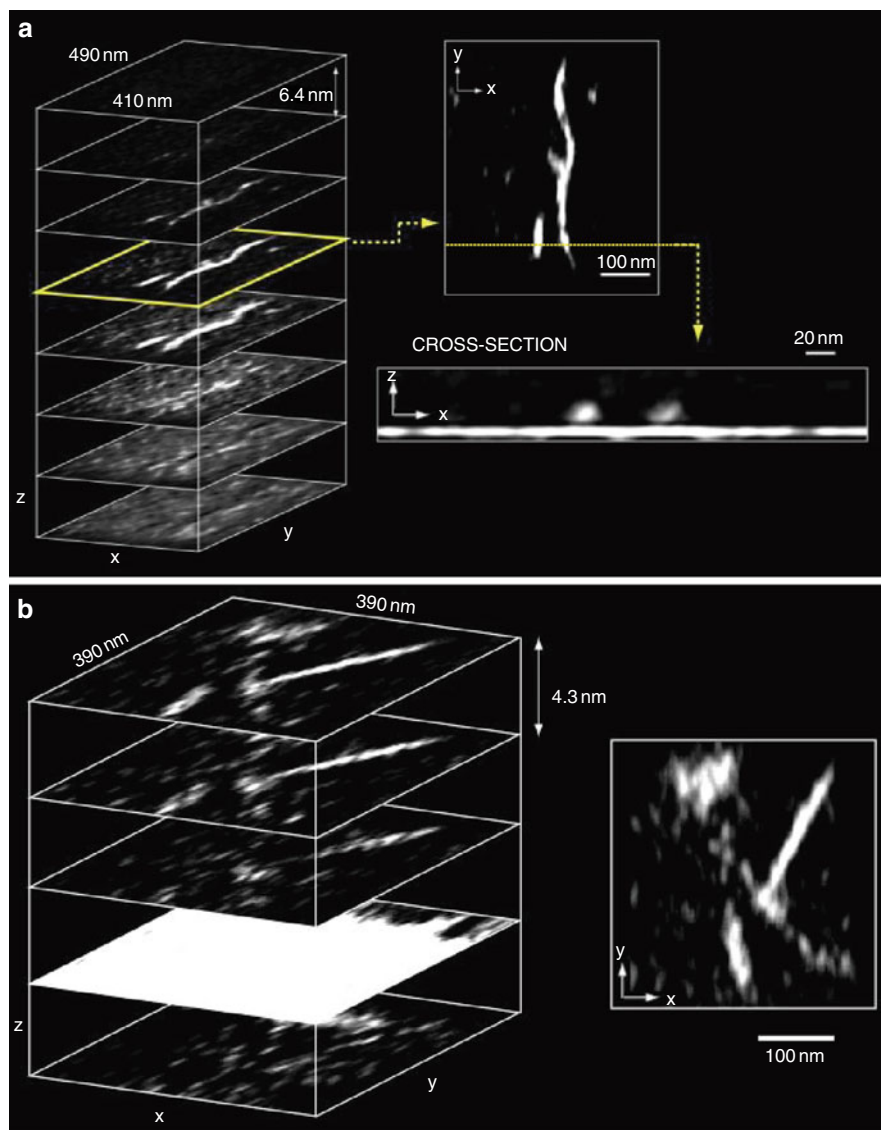
Magnetic Resonance Force Microscopy, Fig. 4 Artistic view of the MRFM apparatus used for MRI of individual tobacco mosaic virus particles. Pictured is the cantilever, the laser beam used for position sensing, and the Cu microwire rf source. The *inset* shows a close-up representation of the gold-coated end of the cantilever with attached virus particles. On *top* of the microwire, is the magnetic FeCo tip with the “mushroom”-shaped resonant slice hovering *above*

cantilever into a droplet of aqueous solution containing suspended TMV. As a result, some TMVs were attached to the gold layer previously deposited on the cantilever end. The density of TMV on the gold layer was low enough that individual particles could be isolated. Then the cantilever was mounted into the low-temperature, ultra-high-vacuum measurement system and aligned over a magnetic tip and rf field source.

After applying a static magnetic field of about 3 T, resonant rf pulses were applied to the rf source in order to flip the ^1H nuclear spins at the cantilever’s mechanical resonance. Finally, the end of the cantilever was mechanically scanned in 3D over the magnetic tip. Given the extended geometry of the region in which the resonant condition is met, i.e., the “resonant slice,” a spatial scan does not directly produce a map of the ^1H distribution in the sample. Instead, each data point in the scan contains force signal from ^1H spins at a variety of different positions. In order to reconstruct the 3D spin density (the MRI image), the force map must be deconvolved by the point spread function defined by the resonant slice. Fortunately, this point spread function can be accurately determined using a magnetostatic model based on the physical geometry of the magnetic tip and the tip magnetization. Deconvolution of the force map into the three-dimensional ^1H spin density can be done in several different ways; for the

Magnetic Resonance Force Microscopy,

Fig. 5 Nanoscale MRI images of tobacco mosaic virus (TMV) particles acquired by MRFM [2]. (a) The series of images *to the left* depicts the 3D ^1H spin density of virus particles deposited on the end of the cantilever. *Black* represents very low or zero density of hydrogen, while *white* is high hydrogen density. The *right side* shows a representative xy -plane, with several viral fragments visible, and a cross section (xz -plane) of two virus particles that reveals an underlying molecular layer of hydrocarbons covering the cantilever surface. (b) 3D ^1H spin density recorded on a different region of the same cantilever as in (a), showing an intact and several fragmented virus particles. The *right side* shows a representative xy -plane



results presented in [2] the authors applied the iterative Landweber deconvolution procedure suggested in an earlier MRFM experiment [25, 26]. This iterative algorithm starts with an initial estimate for the spin density of the object and then improves the estimate successively by minimizing the difference between the measured and predicted spin signal maps. The iterations proceed until the residual error becomes comparable with the measurement noise.

The result of a representative experiment is shown in Fig. 5. Here, clear features of individual TMV particles, which are cylindrical, roughly 300-nm-long and 18 nm in diameter, are visible and can be confirmed

against a scanning electron micrograph (SEM) of the same region. Both whole virus particles and particle fragments are observed. The imaging resolution, while not fine enough to discern any internal structure of the virus particles, constitutes a 1,000-fold improvement over conventional MRI and a corresponding improvement of volume sensitivity by about 100 million.

Comparison to Other Techniques

The unique position of MRFM among high-resolution microscopies becomes apparent when comparing it to

other, more established nanoscale imaging techniques. As a genuine scanning probe method, MRFM has the potential to image matter at atomic resolution. While atomic-scale imaging is routinely achieved in scanning tunneling microscopy and atomic force microscopy, these techniques are confined to the top layer of atoms and cannot penetrate below surfaces [27, 28]. Moreover, in standard scanning probe microscopy (SPM), it is difficult and in many situations impossible to identify the chemical species being imaged. Since MRFM combines SPM and MRI, these restrictions are lifted. The 3D nature of MRI permits acquisition of subsurface images with high spatial resolution even if the probe is relatively far away. As with other magnetic resonance techniques, MRFM comes with intrinsic elemental contrast and can draw from established NMR spectroscopy procedures to perform detailed chemical analysis. In addition, MRI does not cause any radiation damage to samples, as do electron and X-ray microscopies.

MRFM also distinguishes itself from super-resolution optical microscopies that rely on fluorescence imaging [29]. On the one side, optical methods have the advantage of working *in vivo* and they have the ability to selectively target the desired parts of a cell. Fluorescent labeling is now a mature technique which is routinely used for cellular imaging. On the other side, pushing the resolution into the nanometer range is hampered by fundamental limitations, in particular, the high optical powers required and the stability of the fluorophores. Moreover, fluorescent labeling is inextricably linked with a modification of the target biomolecules, which alters the biofunctionality and limits imaging resolution to the physical size of the fluorophores.

MRFM occupies a unique position among other nanoscale spin detection approaches. While single electron spin detection in solids has been shown using several techniques, these mostly rely on the indirect readout via electronic charge [30, 31] or optical transitions [32, 33]. In another approach, the magnetic orientation of single atoms has been measured via the spin-polarized current of a magnetic STM tip or using magnetic exchange force microscopy [34–36]. These tools are very valuable to study single surface atoms; however, they are ill-suited to map out subsurface spins such as paramagnetic defects. In contrast, MRFM *directly* measures the magnetic moment of a spin, without resorting to other degrees of

freedom, making it a very general method. This direct measurement of magnetic moment (or magnetic stray field) could also be envisioned using other techniques, namely, SQuID microscopy [37], Hall microscopy [38], or recently introduced diamond magnetometry based on single nitrogen-vacancy centers [39–41]. So far, however, none of these methods have reached the level of sensitivity needed to detect single electron spins, or volumes of nuclear spins much less than 1 μm [42, 43]. It is certainly possible that future improvements to these methods – especially to diamond magnetometry – may result in alternative techniques for nanoscale MRI that surpass the capabilities of MRFM.

Outlook

Despite the tremendous improvements made to MRFM over the last decade, several important obstacles must be overcome in order to turn the technique into a useful tool for biologists and materials scientists. Most existing MRFM instruments are technically involved prototypes; major hardware simplifications will be required for routine screening of nanoscale samples. Suitable specimen preparation methods must be developed that are compatible with the low-temperature, high-vacuum environment required for the microscope to operate at its highest sensitivity and resolution. While this is particularly challenging for biological samples, protocols exist which could be adapted to MRFM. In cryo-electron microscopy, for example, dispersed samples are vitrified to preserve their native structure by plunge-freezing in liquid nitrogen [44]. As objects become smaller, isolation of samples and suppression of unwanted background signals from surrounding material will become increasingly important.

The conditions under which the latest MRFM imaging experiments were carried out are remarkably similar to those prevailing in cryo-electron microscopy, the highest resolution 3D imaging technique commonly used by structural biologists today. Cryo-electron microscopy, like MRFM, operates at low temperatures and in high vacuum, requires long averaging times (on the order of days) to achieve sufficient contrast, and routinely achieves resolutions of a few nanometers [45, 46]. Unlike MRFM, however, electron microscopy suffers from fundamental

limitations that severely restrict its applicability. Specimen damage by the high-energy electron radiation limits resolution to 5–10 nm if only a single copy of an object is available. Averaging over hundreds to thousands of copies is needed to achieve resolutions approaching 10 Å [47]. In addition, unstained images have intrinsically low contrast, whereas staining comes at the expense of modifying the native structure.

MRFM has the unique capability to image nanoscale objects in a noninvasive manner and to do so with intrinsic chemical selectivity. For this reason the technique has the potential to extend microscopy to the large class of structures that show disorder and therefore cannot be averaged over many copies. These structures include such prominent examples as HIV, influenza virus, and amyloid fibrils. Virtually all of these complexes are associated with important biological functions ranging from a variety of diseases to the most basic tasks within the cellular machinery. For such complexes, MRFM has the potential not only to image the 3D macromolecular arrangement, but also to selectively image specific domains in the interior through isotopic labeling.

While the most exciting prospect for MRFM remains in its application to structural imaging in molecular biology, its applications are not limited to biological matter. For example, most semiconductors contain nonzero nuclear magnetic moments. Therefore, MRFM may prove useful for subsurface imaging of nanoscale electronic devices. MRFM also appears to be the only technique capable of directly measuring the dynamics of the small ensembles of nuclear spin that limit electron spin coherence in single semiconductor quantum dots. Polymer films and self-assembled monolayers – important for future molecular electronics – are another exciting target for MRFM and its capability to image chemical composition on the nanoscale. Finally, isotopically engineered materials are becoming increasingly important for tuning a variety of physical properties such as transport and spin. Researchers currently lack a general method for noninvasively imaging the isotopic composition of these materials [48–50]; MRFM techniques could fill this void.

Thanks to H. J. Mamin and D. Rugar of the IBM Almaden Research Center for their many detailed comments and very helpful discussions pertaining to this text.

Cross-References

- ▶ [Atomic Force Microscopy](#)
- ▶ [Basic MEMS Actuators](#)
- ▶ [Imaging Human Body Down to Molecular Level](#)

References

1. Rugar, D., et al.: Single spin detection by magnetic resonance force microscopy. *Nature* **430**, 329 (2004)
2. Degen, C.L., Poggio, M., Mamin, H.J., Rettner, C.T., Rugar, D.: Nanoscale magnetic resonance imaging. *Proc. Natl. Acad. Sci. U.S.A.* **106**, 1313 (2009)
3. Ciobanu, L., Seeber, D.A., Pennington, C.H.: 3D MR microscopy with resolution by 3.7 μm by 3.3 μm by 3.3 μm . *J. Magn. Reson.* **158**, 178 (2002); Lee, S.-C., et al.: One Micrometer Resolution NMR Microscopy. *J. Magn. Reson.* **150**, 207 (2001); Glover, P., Mansfield, P.: Limits to magnetic resonance microscopy. *Rep. Prog. Phys.* **65**, 1489 (2002)
4. Evans, D.F.: Direct observation of static nuclear susceptibilities at room temperature. *Philos. Mag.* **1**, 370 (1956)
5. Alzetta, G., Arimondo, E., Ascoli, C., Gozzini, A.: Paramagnetic resonance experiments at low fields with angular-momentum detection. *Il Nuovo Cimento B* **62**, 392 (1967)
6. Sidles, J.A.: Noninductive detection of single-proton magnetic resonance. *Appl. Phys. Lett.* **58**, 2854 (1991)
7. Sidles, J.A.: Folded Stern-Gerlach experiment as a means for detecting nuclear magnetic resonance in individual nuclei. *Phys. Rev. Lett.* **68**, 1124 (1992)
8. Rugar, D., Yannoni, C.S., Sidles, J.A.: Mechanical detection of magnetic resonance. *Nature* **360**, 563 (1992)
9. Sidles, J.A., Garbini, J.L., Drobný, G.P.: The theory of oscillator-coupled magnetic resonance with potential applications to molecular imaging. *Rev. Sci. Instrum.* **63**, 3881 (1992)
10. Stipe, B.C., et al.: Magnetic dissipation and fluctuations in individual nanomagnets measured by ultrasensitive cantilever magnetometry. *Phys. Rev. Lett.* **86**, 2874 (2001)
11. Rugar, D., et al.: Force detection of nuclear magnetic resonance. *Science* **264**, 1560 (1994)
12. Wago, K., Züger, O., Kendrick, R., Yannoni, C.S., Rugar, D.: Low-temperature magnetic resonance force detection. *J. Vac. Sci. Technol. B* **14**, 1197 (1996)
13. Mamin, H.J., Budakian, R., Chui, B.W., Rugar, D.: Detection and manipulation of statistical polarization in small spin ensembles. *Phys. Rev. Lett.* **91**, 207604 (2003)
14. Mamin, H.J., et al.: Isotope-selective detection and imaging of organic nanolayers. *Nano Lett.* **9**, 3020 (2009)
15. Sidles, J.A., et al.: Magnetic resonance force microscopy. *Rev. Mod. Phys.* **67**, 249 (1995)
16. Nestle, N., Schaff, A., Veeman, W.S.: Mechanically detected NMR, an evaluation of the applicability for chemical investigations. *Prog. Nucl. Magn. Reson. Spectrosc.* **38**, 1 (2001)

17. Suter, A.: The magnetic resonance force microscope. *Prog. Nucl. Magn. Reson. Spectrosc.* **45**, 239 (2004)
18. Berman, G.P., Borgonovi, F., Gorshkov, V.N., Tsifrinovich, V.I.: *Magnetic Resonance Force Microscopy and a Single-spin Measurement*. World Scientific, Singapore-New Jersey-London-Hong Kong (2006)
19. Hammel, P.C., Pelekhov, D.V.: The magnetic resonance microscope. In: Kronmüller, H., Parkin, S. (eds.) *Handbook of Magnetism and Advanced Magnetic Materials*. Spintronics and magnetoelectronics, vol. 5. John Wiley & Sons, Chichester (2007). ISBN 978-0-470-02217-7
20. Kuehn, S., Hickman, S.A., Marohn, J.A.: Advances in mechanical detection of magnetic resonance. *J. Chem. Phys.* **128**, 052208 (2008)
21. Barbic, M.: Magnetic resonance force microscopy, in magnetic resonance microscopy: spatially resolved NMR techniques and applications. In: Codd, S.L., Seymour, J.D. (eds.) Wiley-VCH Verlag GmbH & Co. KGaA, Weinheim, Germany (2009)
22. Poggio, M., Degen, C.L.: Force-detected nuclear magnetic resonance: recent advances and future challenges. *Nanotechnology* **21**, 342001 (2010)
23. Chui, B.W., et al.: Mass-loaded cantilevers with suppressed higher-order modes for magnetic resonance force microscopy. *TRANSDUCERS, 12th International Conference on Solid-State Sensors, Actuators and Microsystems*, Boston, vol. 2, p. 1120 (2003)
24. Mamin, H.J., Rugar, D.: Sub-attoneutron force detection at millikelvin temperatures. *Appl. Phys. Lett.* **79**, 3358 (2001)
25. Chao, S., Dougherty, W.M., Garbini, J.L., Sidles, J.A.: Nanometer-scale magnetic resonance imaging. *Rev. Sci. Instr.* **75**, 1175 (2004)
26. Dobegeon, N., Hero, A.O., Tourneret, J.-Y.: Hierarchical bayesian sparse image reconstruction with application to MRFM. *IEEE Trans. Image Process.* **18**, 2059 (2009)
27. Hansma, P., Tersoff, J.: Scanning tunneling microscopy. *J. Appl. Phys.* **61**, R1–R23 (1987)
28. Giessibl, F.: Advances in atomic force microscopy. *Rev. Mod. Phys.* **75**, 949–983 (2003)
29. Huang, B., Bates, M., Zhuang, X.: Super-resolution fluorescence microscopy. *Annu. Rev. Biochem.* **78**, 993–1016 (2009)
30. Elzerman, J.M., et al.: Single-shot read-out of an individual electron spin in a quantum dot. *Nature* **430**, 431 (2004)
31. Xiao, M., Martin, I., Yablonovitch, E., Jiang, H.W.: Electrical detection of the spin resonance of a single electron in a silicon field-effect transistor. *Nature* **430**, 435 (2004)
32. Wrachtrup, J., von Borczyskowski, C., Bernard, J., Orritt, M., Brown, R.: Optical detection of magnetic resonance in a single molecule. *Nature* **363**, 244 (1993)
33. Jelezko, F., Popa, I., Gruber, A., Tietz, C., Wrachtrup, J.: Single spin states in a defect center resolved by optical spectroscopy. *Appl. Phys. Lett.* **81**, 2160 (2002)
34. Heinze, S., et al.: Real-space imaging of two-dimensional antiferromagnetism on the atomic scale. *Science* **288**, 1805–1808 (2000)
35. Durkan, C., Welland, M.E.: Electronic spin detection in molecules using scanning-tunneling- microscopy-assisted electron-spin resonance. *Appl. Phys. Lett.* **80**, 458 (2002)
36. Kaiser, U., Schwarz, A., Wiesendanger, R.: *Nature* **446**, 522–525 (2007)
37. Kirtley, J.R., et al.: High-resolution scanning SQUID microscope. *Appl. Phys. Lett.* **66**, 1138 (1995)
38. Chang, A.M., et al.: Scanning hall probe microscopy. *Appl. Phys. Lett.* **61**, 1974 (1992)
39. Degen, C.L.: Scanning magnetic field microscope with a diamond single-spin sensor. *Appl. Phys. Lett.* **92**, 243111 (2008)
40. Maze, J.R., et al.: Nanoscale magnetic sensing with an individual electronic spin in diamond. *Nature* **455**, 644 (2008)
41. Balasubramanian, G., et al.: Nanoscale imaging magnetometry with diamond spins under ambient conditions. *Nature* **455**, 648 (2008)
42. Degen, C.L.: Nanoscale magnetometry: microscopy with single spins. *Nat. Nanotechnol.* **3**, 643 (2008)
43. Blank, A., Suhovoy, E., Halevy, R., Shtirberg, L., Harneit, W.: ESR imaging in solid phase down to sub-micron resolution: methodology and applications. *Phys. Chem. Chem. Phys.* **11**, 6689–6699 (2009)
44. Taylor, K.A., Glaeser, R.M.: Electron diffraction of frozen, hydrated protein crystals. *Science* **186**, 1036 (1974)
45. Lucic, V., Forster, F., Baumeister, W.: Structural studies by electron tomography: from cells to molecules. *Annu. Rev. Biochem.* **74**, 833 (2005)
46. Subramaniam, S.: Bridging the imaging gap: visualizing subcellular architecture with electron tomography. *Curr. Opin. Microbiol.* **8**, 316 (2005)
47. Glaeser, R.M.: Cryo-electron microscopy of biological nanostructures. *Phys. Today* **61**, 48 (2008)
48. Shimizu, Y., Itoh, K.: Growth and characterization of short-period silicon isotope superlattices. *Thin Solid Films* **508**, 160–162 (2006)
49. Shlimak, I., Safarov, V., Vagner, I.: Isotopically engineered silicon/silicon-germanium nanostructures as basic elements for a nuclear spin quantum computer. *J. Phys. Cond. Matter* **13**, 6059 (2001)
50. Kelly, T., Miller, M.: Atom probe tomography. *Rev. Sci. Instrum.* **78**, 031101 (2007)

Magnetic Self-Assembly

► Magnetic-Field-Based Self-Assembly

Magnetic-Field-Based Self-Assembly

Li Zhang¹, Bradley J. Nelson¹ and Lixin Dong²

¹Institute of Robotics and Intelligent Systems, ETH Zurich, Zurich, Switzerland

²Electrical and Computer Engineering, Michigan State University, East Lansing, MI, USA

Synonyms

Magnetic assembly; Magnetic self-assembly